

PION POLARIZABILITIES

L.V. Fil'kov and V.L. Kashevarov

Lebedev Physical Institute, Leninsky Prospect 53, 119991 Moscow, Russia

1 Introduction

Pion polarizabilities are fundamental structure parameters characterizing the behavior of the pion in an external electromagnetic field. The dipole and quadrupole polarizabilities are defined [1, 2] through the expansion of the non-Born helicity amplitudes of the Compton scattering on the pion over t at the fixed $s = \mu^2$

$$\begin{aligned} M_{++}(s = \mu^2, t) &= \pi\mu \left[2(\alpha_1 - \beta_1) + \frac{t}{6}(\alpha_2 - \beta_2) \right] + \mathcal{O}(t^2), \\ M_{+-}(s = \mu^2, t) &= \frac{\pi}{\mu} \left[2(\alpha_1 + \beta_1) + \frac{t}{6}(\alpha_2 + \beta_2) \right] + \mathcal{O}(t^2), \end{aligned} \quad (1)$$

where s (t) is the square of the total energy (momentum transfer) in the $\gamma\pi$ c.m. system and μ is the pion mass. The dipole electric (α_1) and magnetic (β_1) pion polarizabilities measure the response of the pion to quasistatic electric and magnetic fields. On the other hand, the parameters α_2 and β_2 measure the electric and magnetic quadrupole moments induced in the pion in the presence of an applied field gradient. In the following the dipole and quadrupole polarizabilities are given in units 10^{-4}fm^3 and 10^{-4}fm^5 , respectively.

The values of the pion polarizabilities are very sensitive to predictions of different theoretical models. Therefore, an accurate experimental determination of these parameters are very important for testing the validity of such models.

By now the values of the pion polarizabilities were determined by analysing processes $\pi^- A \rightarrow \gamma\pi^- A$, $\gamma p \rightarrow \gamma\pi^+ n$, and $\gamma\gamma \rightarrow \pi\pi$. In the present work we mainly analyse the results obtained in recent works [2–5]

2 π^0 meson polarizabilities

At present the most reliable method of a determination of the π^0 meson polarizabilities is an analysis of the process $\gamma\gamma \rightarrow \pi^0\pi^0$ in the energy region up to ~ 2 GeV where the cross section of this process is very sensitive to the values of the π^0 polarizabilities. This process is described by the following invariant variables:

$$t = (k_1 + k_2)^2, \quad s = (q_1 - k_1)^2, \quad u = (q_1 - k_2)^2, \quad (2)$$

where $q_1(q_2)$ and $k_1(k_2)$ are the pion and photon four-momenta. The cross section of the process $\gamma\gamma \rightarrow \pi^0\pi^0$ is expressed through the helicity amplitudes as follows

$$\frac{d\sigma_{\gamma\gamma \rightarrow \pi^0\pi^0}}{d\Omega} = \frac{1}{256\pi^2} \sqrt{\frac{(t - 4\mu^2)}{t^3}} \left\{ t^2 |M_{++}|^2 + \frac{1}{16} t^2 (t - 4\mu^2)^2 \sin^4 \theta^* |M_{+-}|^2 \right\}, \quad (3)$$

where θ^* is the angle between the photon and the pion in the c.m.s. of the process under consideration.

In order to analyse the process $\gamma\gamma \rightarrow \pi^0\pi^0$ we constructed dispersion relations (DRs) at fixed t with one subtraction at $s = \mu^2$ for the helicity amplitude $M_{++}(s, t)$ [2]

$$ReM_{++}(s, t) = ReM_{++}(s = \mu^2, t) + \frac{(s - \mu^2)}{\pi} P \int_{4\mu^2}^{\infty} ds' ImM_{++}(s', t) \left[\frac{1}{(s' - s)(s' - \mu^2)} - \frac{1}{(s' - u)(s' - \mu^2 + t)} \right]. \quad (4)$$

Via the cross symmetry these DRs are identical to DRs with two subtractions. The subtraction function $ReM_{++}(s = \mu^2, t)$ was determined with the help of the DRs at fixed $s = \mu^2$ with two subtractions using the cross symmetry between the s and u channels

$$ReM_{++}(s = \mu^2, t) = M_{++}(s = \mu^2, 0) + t \frac{dM_{++}(s = \mu^2, t)}{dt} \Big|_{t=0} + \frac{t^2}{\pi} \left\{ P \int_{4\mu^2}^{\infty} \frac{ImM_{++}(t', s = \mu^2) dt'}{t'^2(t' - t)} + \int_{4\mu^2}^{\infty} \frac{ImM_{++}(s', u = \mu^2) ds'}{(s' - \mu^2)^2(s' - \mu^2 + t)} \right\}. \quad (5)$$

The DRs for the amplitude $M_{+-}(s, t)$ had the same expressions (4) and (5) with substitutions: $M_{++} \rightarrow M_{+-}$ and $ImM_{++} \rightarrow ImM_{+-}$.

The subtraction constants were expressed through the sum and the difference of the electric and magnetic polarizabilities taking into account Eq. (1):

$$M_{++}(s = \mu^2, t = 0) = 2\pi\mu(\alpha_1 - \beta_1)_{\pi^0}, \quad \frac{dM_{++}(s = \mu^2, t)}{dt} \Big|_{t=0} = \frac{\pi\mu}{6}(\alpha_2 - \beta_2)_{\pi^0}, \quad (6)$$

$$M_{+-}(s = \mu^2, t = 0) = \frac{2\pi}{\mu}(\alpha_1 + \beta_1)_{\pi^0}, \quad \frac{dM_{+-}(s = \mu^2, t)}{dt} \Big|_{t=0} = \frac{\pi}{6\mu}(\alpha_2 + \beta_2)_{\pi^0}. \quad (7)$$

These DRs were used to fit the experimental data to the total cross section of the process $\gamma\gamma \rightarrow \pi^0\pi^0$. The DRs were saturated by the contribution of $\rho(770)$, $\omega(782)$, and $\phi(1020)$ mesons in the s channel and σ , $f_0(980)$, $f_0(1370)$, $f_2(1270)$, and $f_2(1525)$ in t channel. The polarizabilities $(\alpha_1 \pm \beta_1)_{\pi^0}$ and $(\alpha_2 \pm \beta_2)_{\pi^0}$ and parameters of the σ meson were considered as free parameters.

For the reaction under consideration the Born term is equal to zero and the main contribution in the energy region $\sqrt{t} = 270\text{--}825$ MeV is determined by S wave. So, this process gives a good possibility to search for the σ meson. The parameters of such a σ meson and the values of the dipole polarizabilities have been found from the fit to the experimental data [6] in the energy regions 270–825 MeV and 270–2000 MeV, respectively [3]. The values of the quadrupole polarizabilities have been determined from the fit to experimental data [6, 7] in the energy region 270–2250 MeV [2].

The result of the fit to the experimental data for the total cross section [6, 7] in the energy region from threshold to 2250 MeV is presented in Fig. 1 by solid curve [2]. The dashed curve corresponds to the quadrupole polarizabilities calculated with the help of the dispersion sum rules (DSRs) from Ref. [2]. The full circles are data from Ref. [6] and the open ones are data from Ref. [7].

The following parameters of the σ meson have been determined in the Ref. [3]: $m_\sigma = 547 \pm 45$ MeV, $\Gamma_\sigma = 1204 \pm 362$ MeV, $\Gamma_{\sigma \rightarrow \gamma\gamma} = 0.62 \pm 0.19$ keV. This value of $\Gamma_{\sigma \rightarrow \gamma\gamma}$ differs strongly from the result of Ref. [8] [$\Gamma_{\sigma \rightarrow \gamma\gamma} = (3.8 \pm 1.5)$ keV]. It should be noted that the

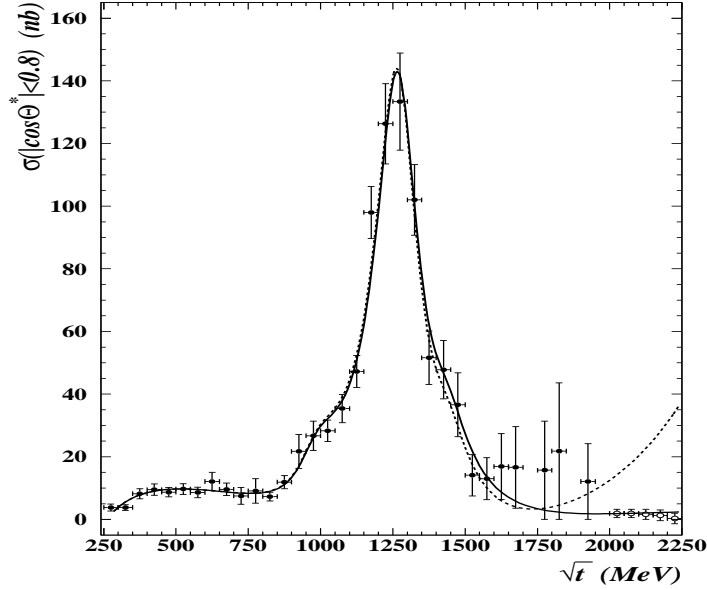


Figure 1: The total cross section of the reaction $\gamma\gamma \rightarrow \pi^0\pi^0$.

Table 1: The dipole and quadrupole polarizabilities of the π^0 meson

	fit	DSRs [2]	ChPT
$(\alpha_1 - \beta_1)_{\pi^0}$	-1.6 ± 2.2 [3] -0.6 ± 1.8 [9]	-3.49 ± 2.13	-1.9 ± 0.2 [11]
$(\alpha_1 + \beta_1)_{\pi^0}$	0.98 ± 0.03 [3] 1.00 ± 0.05 [10]	0.802 ± 0.035	1.1 ± 0.3 [11]
$(\alpha_2 - \beta_2)_{\pi^0}$	39.70 ± 0.02 [2]	39.72 ± 8.01	37.6 ± 3.3 [12]
$(\alpha_2 + \beta_2)_{\pi^0}$	-0.181 ± 0.004 [2]	-0.171 ± 0.067	0.04 [12]

use of the value of $\Gamma_{\sigma \rightarrow \gamma\gamma} = (3.8 \pm 1.5)$ keV in the analysis [2] leads to a strong deviation from the experimental data on the total cross section of the process under consideration.

The values of the dipole and quadrupole polarizabilities found in the fits [2,3] are listed in Table 1 together with results obtained in Refs. [9,10] and prediction of DSRs [2] and two loop calculations in the frame of ChPT [11,12]. The obtained values of the sum and difference of the dipole polarizabilities of π^0 and the difference of its quadrupole polarizabilities do not conflict within the errors with the predictions of DSRs and ChPT. However, there are very big errors in the experimental values for the difference of the dipole polarizabilities. Therefore, it is difficult to do a more unambiguous conclusion. As for the sum of the quadrupole polarizabilities of π^0 , the DSR result agrees well with the experimental value, but the ChPT predicts a positive value in contrast to experimental result. However, as it was noted in Ref. [12], this quantity was obtained in a two-loop approximation, which is a leading order result for this sum, and one expects substantial corrections to it from three-loop calculations.

It should be noted that the values of the difference and the sum of the quadrupole polarizabilities found from the fit have very small errors. They are the errors of the fitting. This is a result of a very high sensitivity of the total cross section of the process $\gamma\gamma \rightarrow \pi^0\pi^0$ at $\sqrt{t} > 1500$ MeV to values of these parameters. In order to estimate real values of errors of these difference and sum, model errors should be added.

3 Measurement of the π^+ meson polarizabilities via the $\gamma p \rightarrow \gamma \pi^+ n$ reaction

The pion polarizability can be extracted from experimental data on radiative pion photoproduction, either by extrapolating these data to the pion pole [13–16], or by comparing the experimental cross section with the predictions of different theoretical models. The extrapolation method was first suggested in [17] and has been widely used for the determination of cross sections and phase shifts of elastic $\pi\pi$ -scattering from the reaction $\pi N \rightarrow \pi\pi N$. For investigations of $\gamma\pi^+$ -scattering this method was first used in [18, 19].

However, in order to obtain a reliable value of the pion polarizability, it is necessary to obtain the experimental data on pion radiative photoproduction with small errors over a sufficiently wide region of t , in particular very close to $t = 0$ [20, 21].

It should be noted that there is an essential difference in extrapolating the data of the processes $\pi N \rightarrow \pi\pi N$ and $\gamma p \rightarrow \gamma\pi N$. In the former case, the pion pole amplitude gives the main contribution in a certain energy region. This permits one to constrain the extrapolation function to be zero at $t = 0$ providing a precise determination of the amplitude. In the case of radiative pion photoproduction, the pion pole amplitude alone is not gauge invariant and we must take into account all pion and nucleon pole amplitudes. However, the sum of these amplitudes does not vanish at $t = 0$. This complicates the extrapolation procedure by increasing the requirements on the accuracy of the experimental data.

As the accuracy of the data [4] was not sufficient for a reliable extrapolation, the values of the pion polarizabilities have been obtained from a fit of the cross section calculated by different theoretical models to the data.

The theoretical calculations of the cross section for the reaction $\gamma p \rightarrow \gamma \pi^+ n$ showed that the contribution of nucleon resonances is suppressed for photons scattered backward in the c.m.s. of the reaction $\gamma\pi \rightarrow \gamma\pi$. Moreover, integration over φ and $\theta_{\gamma\gamma'}^{cm}$ essentially decreases the contribution of resonances from the crossed channels. On the other hand, the difference $(\alpha_1 - \beta_1)_{\pi^+}$ gives the biggest contribution to the cross section for $\theta_{\gamma\gamma'}^{cm}$ in the region of $140^\circ - 180^\circ$. Therefore, we considered the cross section of radiative pion photoproduction integrated over φ from 0° to 360° and over $\theta_{\gamma\gamma'}^{cm}$ from 140° to 180° ,

$$\int_0^{360^\circ} d\varphi \int_{-1}^{-0.766} d\cos\theta_{\gamma\gamma'}^{cm} \frac{d\sigma_{\gamma p \rightarrow \gamma \pi^+ n}}{dt ds_1 d\Omega_{\gamma\gamma'}}, \quad (8)$$

where $s_1 = (q_1 + k_1)^2$ is the square of the total energy in c.m. system for the $\gamma\pi \rightarrow \gamma\pi$ reaction, $t = (p_p - p_n)^2 \simeq -2mT_n$ is the square of the momentum transfer for the $\gamma p \rightarrow \gamma \pi^+ n$ reaction and T_n is the kinetic energy of the neutron.

The cross section of the process $\gamma p \rightarrow \gamma \pi^+ n$ has been calculated in the framework of two different models. In the first model (model-1) the contribution of all the pion and nucleon pole diagrams was taken into account using pseudoscalar pion-nucleon coupling [22].

The second model (model-2) included the nucleon and the pion pole diagrams without the anomalous magnetic moments of the nucleons, and in addition the contributions of the resonances $\Delta(1232)$, $P_{11}(1440)$, $D_{13}(1520)$, $S_{11}(1535)$, and σ meson.

The experiment on the radiative π^+ meson photoproduction was carried out at the Mainz Microtron MAMI in the energy region $537 \text{ MeV} < E_\gamma < 817 \text{ MeV}$.

To increase our confidence that the model dependence of the result was under control we limited ourselves to kinematic regions where the difference between model-1 and model-2 did not exceed 3% when $(\alpha_1 - \beta_1)_{\pi^+}$ was constrained to zero. First, the kinematic region, where

the contribution of the pion polarizability is negligible, i.e. the region $1.5\mu^2 \leq s_1 < 5\mu^2$, was considered.

In Fig. 2, the experimental data for the differential cross section, averaged over the full

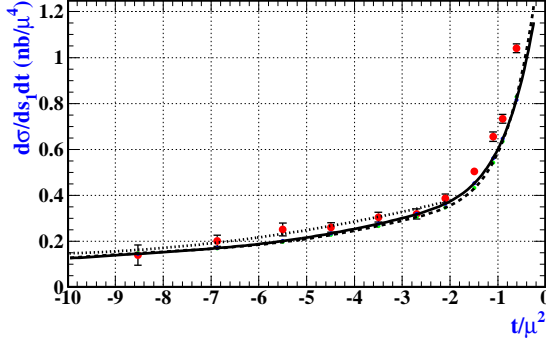


Figure 2: The differential cross section of the process $\gamma p \rightarrow \gamma \pi^+ n$ averaged over the full photon beam energy interval and over s_1 from $1.5\mu^2$ to $5\mu^2$

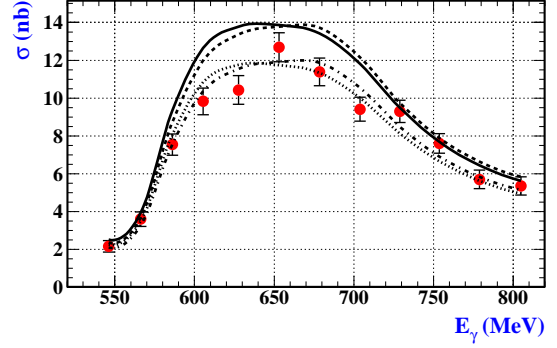


Figure 3: The differential cross section of the process $\gamma p \rightarrow \gamma \pi^+ n$ integrated over s_1 and t in the region, where the contribution of the pion polarizability is biggest.

photon beam energy interval from 537 MeV up to 817 MeV and over s_1 in the indicated interval, are compared to predictions of model-1 (dashed curve) and model-2 (solid curve). The dotted curve is the fit of the experimental data in the region of $-10\mu^2 < t < -2\mu^2$. As seen from this figure, the theoretical curves are very close to the experimental data. The small difference between the theoretical curves and the experimental data was used for a normalization of the experimental data.

Then we investigated the kinematic region where the polarizability contribution is biggest. This is the region $5\mu^2 \leq s_1 < 15\mu^2$ and $-12\mu^2 < t < -2\mu^2$. In the range $t > -2\mu^2$ the polarizability contribution is small and also the efficiency of the TOF is not well known here. Therefore, we have excluded this region. Fig. 3 presents the cross section of the process $\gamma p \rightarrow \gamma \pi^+ n$ integrated over s_1 and t in the region where the contribution of the pion polarizabilities is biggest and the difference between of the theoretical models does not exceed 3%. The dashed and dashed-dotted lines are the predictions of model-1 and the solid and dotted lines of model-2 for $(\alpha_1 - \beta_1)_{\pi^+} = 0$ and 14, respectively. As a result, the following value of the difference of the charged pion dipole polarizabilities has been obtained:

$$(\alpha_1 - \beta_1)_{\pi^+} = 11.6 \pm 1.5_{stat} \pm 3.0_{syst} \pm 0.5_{mod}. \quad (9)$$

4 Determination of the charged pion polarizabilities from the process $\gamma\gamma \rightarrow \pi^+\pi^-$

Attempts to determine the charge pion dipole polarizabilities from the reaction $\gamma\gamma \rightarrow \pi^+\pi^-$ suffered greatly from theoretical and experimental uncertainties. The analyses [9,23,24] have been performed in the region of the low energy ($\sqrt{t} < 700$ MeV, where t is the square of the total energy in $\gamma\gamma$ c.m.system). In this region values of the experimental cross sections of

the process under consideration [25–28] are very ambiguous. As a result, the values of $\alpha_{1\pi^\pm}$ found lie in the interval 2.2–26.3. The analyses of the data of Mark II [28] have given $\alpha_{1\pi^\pm}$ close to ChPT result. However, even changes of the dipole polarizabilities by more than 100% are still compatible with the present error bars in the energy region considered [24].

In the work [5] we constructed the DRs similar to those of Ref. [2] for the amplitudes of the process $\gamma\gamma \rightarrow \pi^+\pi^-$. But in this case the Born term does not equal to 0. Using the DRs allows one to avoid the problem of double counting and the subtractions in the DRs provide a good convergence of the integrand expressions of these DRs and, therefore, increases the reliability of the calculations. The DRs for the charged pions are saturated by the contributions of the $\rho(770)$, $b_1(1235)$, $a_1(1260)$, and $a_2(1320)$ mesons in the s channel and σ , $f_0(980)$, $f_0(1370)$, $f_2(1270)$, and $f_2(1525)$ in the t channel.

These DRs, where the charged pion dipole and quadrupole polarizabilities were free parameters, were used to fit to the experimental data for the total cross section [28–33] in energy region from threshold to 2500 MeV. The best result of this fit is presented in Fig. 4 by the solid line. This solid curve well describes the experimental data in whole energy

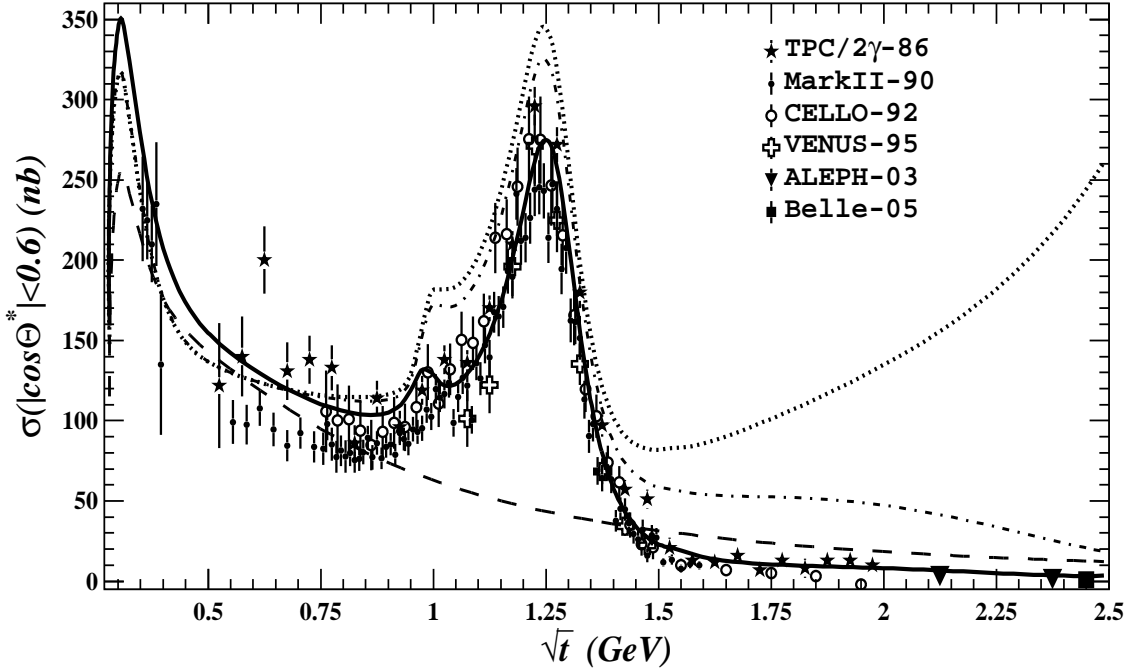


Figure 4: The total cross section of for the reaction $\gamma\gamma \rightarrow \pi^+\pi^-$ (with $|\cos \theta^*| < 0.6$).

region under investigation. As a result, we have found the dipole polarizabilities of the charged pions and determined their quadrupole polarizabilities for the first time. The values of the polarizabilities found in the work [5] and the predictions of DSRs [2] and two-loop ChPT [34] are listed in Table 2. The numbers in brackets correspond to the order p^6 low energy constants from Ref. [35]. As seen from this Table, the all values of polarizabilities found in Ref. [5] are in good agreement with the DSR predictions [2].

The dashed curve in Fig. 4 is the Born term contribution. The dotted curve is a result of calculations using the DRs when $(\alpha_2 - \beta_2)_{\pi^\pm}$ and $(\alpha_2 + \beta_2)_{\pi^\pm}$ equal to the respective values in Table 2. but the dipole polarizabilities are taken from ChPT calculations [36] as $(\alpha_1 - \beta_1)_{\pi^\pm} = 4.4$ and $(\alpha_1 + \beta_1)_{\pi^\pm} = 0.3$. The dashed-dotted curve presents a result of the fit to the experimental data when the quadrupole polarizabilities are the free parameters and the values of the dipole polarizabilities are fixed by ChPT calculations [36]. The both last

Table 2: The dipole and quadrupole polarizabilities of the charged pions.

	fit [5]	DSRs [2]	ChPT [34]	
			to one-loop	to two-loops
$(\alpha_1 - \beta_1)_{\pi^\pm}$	$13.0^{+2.6}_{-1.9}$	13.60 ± 2.15	6.0	5.7 [5.5]
$(\alpha_1 + \beta_1)_{\pi^\pm}$	$0.18^{+0.11}_{-0.02}$	0.166 ± 0.024	0	0.16 [0.16]
$(\alpha_2 - \beta_2)_{\pi^\pm}$	$25.0^{+0.8}_{-0.3}$	25.75 ± 7.03	11.9	16.2 [21.6]
$(\alpha_2 + \beta_2)_{\pi^\pm}$	0.133 ± 0.015	0.121 ± 0.064	0	-0.001 [-0.001]

curves are close to calculations in Ref. [24] in the energy region up to 700 MeV, however they differ strongly from all experimental data on the total cross section at higher energies.

The fits of the data to the total cross section for the separate works [28–31] were used to estimate the errors of the values of charged pion polarizabilities found.

The angular distributions of the differential cross section of the process $\gamma\gamma \rightarrow \pi^+\pi^-$ at different energies are shown in Fig. 5. The solid and dashed curves are the results of

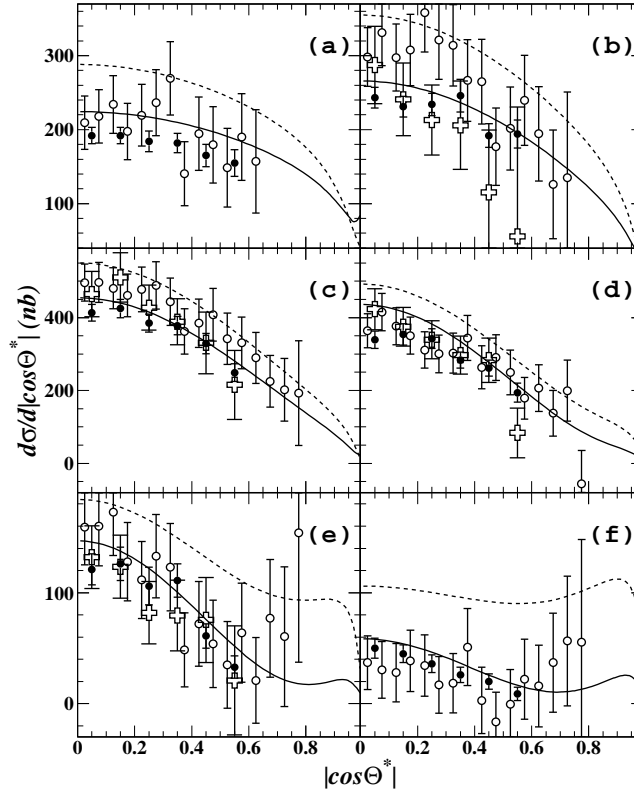


Figure 5: Angular distributions of the differential cross sections for the following energy intervals: (a) – 0.95–1.05 GeV, (b) – 1.05–1.15 GeV, (c) – 1.15–1.25 GeV, (d) – 1.25–1.35 GeV, (e) – 1.35–1.45 GeV, (f) – 1.45–1.55 GeV. The designations of the experimental data are the same as in Fig. 4.

calculations using our and the ChPT fits (the latter when the values of the dipole polarizabilities are fixed by ChPT [36]) to the total cross sections in Fig. 4, respectively. This figure demonstrates a good description of the angular distributions by the solid curves with the polarizability values found in the present work. On the other hand, the calculations with the dipole polarizabilities from ChPT [36] contradict these experimental data, particularly at higher energies.

Table 3: The experimental data on $(\alpha_1 - \beta_1)_{\pi^\pm}$. In [23, 24, 37], $(\alpha_1 - \beta_1)_{\pi^\pm}$ was determined by using a constraint $\alpha_{1\pi^\pm} = -\beta_{1\pi^\pm}$.

Experiments	$(\alpha_1 - \beta_1)_{\pi^\pm}$
L.V. Fil'kov, V.L. Kashevarov (2006) [5] $\gamma\gamma \rightarrow \pi^+\pi^-$: MARK II [28], TPC/2g [29], CELLO [30], VENUS [31], ALEPH [32], BELLE [33]	$13.0^{+2.6}_{-1.9}$
$\gamma p \rightarrow \gamma\pi^+n$: MAMI (2005) [4]	$11.6 \pm 1.5_{stat} \pm 3.0_{syst} \pm 0.5_{mod}$
A.E. Kaloshin, V.V. Serebryakov (1994) [9] $\gamma\gamma \rightarrow \pi^+\pi^-$: MARK II [28]	5.25 ± 0.95
J.F. Donoghue, B.R. Holstein (1993) [24] $\gamma\gamma \rightarrow \pi^+\pi^-$: Mark II [28]	5.4
D. Babusci <i>et al.</i> (1992) [23] $\gamma\gamma \rightarrow \pi^+\pi^-$: PLUTO [25] DM 1 [26] DM 2 [27] Mark II [28]	$38.2 \pm 9.6 \pm 11.4$ 34.4 ± 9.2 52.6 ± 14.8 4.4 ± 3.2
$\gamma p \rightarrow \gamma\pi^+n$: Lebedev Phys.Inst. (1984) [18]	40 ± 24
$\pi^- Z \rightarrow \gamma\pi^- Z$: Serpukhov (1983) [37]	$13.6 \pm 2.8 \pm 2.4$

5 Discussion

The experimental information available so far for the difference of the dipole polarizabilities of charged pions is summarized in Table 3.

The difference of the dipole polarizabilities of charged pions found from the analysis of the process $\gamma\gamma \rightarrow \pi^+\pi^-$ [5] agrees very well with results obtained from the scattering of high energy π^- mesons off the Coulomb field of heavy nuclei [37] and from the radiative photoproduction of π^+ from the proton at MAMI [4] and in Lebedev Physical Institute [18] (see Table 3). However, these values of $(\alpha_1 - \beta_1)_{\pi^\pm}$ deviate substantially from the calculations in the framework of ChPT [34, 36].

The analyses [9] and [24] of the data of MARK II [28] have given the values of $(\alpha_1 - \beta_1)_{\pi^\pm}$ close to the ChPT result. However, they have been determined in the energy region $\sqrt{t} < 700$ MeV, where these data have big errors. Moreover, these small values lead to the strong deviation from the experimental data at higher energies (see Fig. 4).

One of the possible reasons for the small value of $(\alpha_1 - \beta_1)_{\pi^\pm}$ predicted by ChPT could be the neglect of the contribution of the σ meson. As has been shown in Ref. [2], this resonance gives the main contribution to DSRs for $(\alpha_1 - \beta_1)_{\pi^\pm}$.

The difference of the quadrupole polarizabilities $(\alpha_2 - \beta_2)_{\pi^\pm}$ (see Table 2) disagrees with the present two-loop ChPT calculations [34]. One of the sources of such a disagreement is a poor knowledge of low energy constants. Moreover, it should be noted that in this case the two-loop calculation generates nearly a 100% contribution as compared to one-loop result.

Calculations of $(\alpha_{1,2} + \beta_{1,2})$ at order p^6 determine only the leading order term in ChPT. Therefore, contributions at p^8 could be essential, and considerably more work required to put the ChPT prediction on a firm basis [34].

6 Summary

We have reviewed and analysed the data on the pion polarizabilities obtained.

1. The values of the dipole and quadrupole polarizabilities of π^0 have been obtained from the fit of the experimental data [6,7] to the total cross section of the process $\gamma\gamma \rightarrow \pi^0\pi^0$ in the energy region from threshold to 2250 MeV. The values of $(\alpha_1 \pm \beta_1)_{\pi^0}$ and $(\alpha_2 - \beta_2)_{\pi^0}$ do not conflict within the errors with the ChPT prediction. However, two-loop ChPT calculations have given opposite sign for the $(\alpha_2 + \beta_2)_{\pi^0}$.

2. The value of $(\alpha_1 - \beta_1)_{\pi^\pm}$ found in Ref. [5] from the fit of all available at present experimental data to the total cross section (with $|\cos\theta^*| < 0.6$) of the process $\gamma\gamma \rightarrow \pi^+\pi^-$ in the energy region from threshold to 2500 MeV is consisted with the results obtained at MAMI (2005) ($\gamma p \rightarrow \gamma\pi^+n$), in Serpukhov (1983) ($\pi^-Z \rightarrow \gamma\pi^-Z$) and Lebedev Physical Institute (1984) ($\gamma p \rightarrow \gamma\pi^+n$). However, all these results are at variance with the ChPT calculations.

3. The values of the quadrupole polarizabilities $(\alpha_2 \pm \beta_2)_{\pi^\pm}$ found disagree with the present two-loop ChPT calculations.

4. All values of the pion polarizabilities found in Refs. [2–5, 18, 37] agree with DSR predictions.

This research is part of the EU integrated initiative hadron physics project under contract number RII3-CT-2004-506078 and was supported in part by the Russian Foundation for Basic Research (Grant No. 05-02-04014).

References

- [1] I. Guiasu and E.E. Radescu, Ann. Phys. **120**, 145 (1979); *ibid.* **122**, 436 (1979).
- [2] L.V. Fil'kov and V.L. Kashevarov, Phys. Rev. C **72**, 035211 (2005).
- [3] L.V. Fil'kov and V.L. Kashevarov, Eur. Phys. J. A **5**, 285 (1999).
- [4] J. Ahrens *et al.*, Eur. Phys. J. A **23**, 113 (2005).
- [5] L.V. Fil'kov and V.L. Kashevarov, Phys. Rev. C **73**, 035210 (2006).
- [6] H. Marsiske *et al.*, Phys. Rev. D **41**, 3324 (1990).
- [7] J.K. Bienlein, Crystal Ball Contribution to the 9th Intern. Workshop on Photon-Photon Collisions, San Diego, California, 22-26 March 1992.
- [8] M. Boglione, M.R. Pennington, Eur. Phys. J. C **9**, 11 (1999).
- [9] A.E. Kaloshin and V.V. Serebryakov, Z. Phys. C **64**, 689 (1994).
- [10] A.E. Kaloshin, V.M. Persikov, and V.V. Serebryakov, Phys. Atom. Nucl. **57**, 2207 (1994).
- [11] S. Bellucci, J. Gasser, and M.E. Sainio, Nucl. Phys. **B423**, 80 (1994); **B431**, 413 (1994).
- [12] J. Gasser, M.A. Ivanov, and M.E. Sainio, Nucl. Phys. **728**, 31 (2005).
- [13] L.V. Fil'kov, Proc. Lebedev. Phys. Inst. **41**, 1 (1967).

- [14] T.A. Aibergenov *et al.*, Proc. Lebedev Phys. Inst. **186** 169 (1988)
- [15] D. Drechsel and L.V. Fil'kov, Z. Phys. A **349**, 177 (1994).
- [16] Th. Walcher, in Chiral Dynamics: Theory and Experiment III, Proceedings from the Institute for Nuclear Theory, Vol. **11**, p.296.
- [17] G. Gobel, Phys. Rev. Lett. **1**, 337 (1958); G.F. Chew and F.E. Low, Phys. Rev. **113**, 1640 (1959).
- [18] T.A. Aibergenov *et al.* Sov. Phys.-Lebedev Inst. Rep. **6**, 32 (1984); Czech. J. Phys. B **36**, 948 (1986).
- [19] T.A. Aibergenov *et al.*, Sov. Phys-Lebedev Inst. Rep. **5**, 28 (1982).
- [20] J. Ahrens *et al.*, Few-Body Syst. Suppl. **9**, 449 (1995).
- [21] J. Ahrens *et al.*, Preprint of Lebedev Phys. Inst. No. **52** (1996).
- [22] Ch. Uhmeier, PhD Thesis, Mainz University (2000).
- [23] D. Babusci *et al.*, Phys. Lett. **B277**, 158 (1992).
- [24] J.F. Donoghue and B.R. Holstein, Phys. Rev. D **48**, 137 (1993).
- [25] PLUTO Collaboration (C. Berger *et al.*), Z. Phys. C **26** 199 (1984).
- [26] DM1 Collaboration (A. Courau *et al.*), Nucl. Phys. B **271**, 1 (1986).
- [27] DM2 Collaboration (Z. Ajaltoni *et al.*), Phys. Lett. **B194**, 573 (1987).
- [28] Mark II Collaboration (J. Boyer *et al.*), Phys. Rev. D **42**, 1350 (1990).
- [29] TPC/2 γ Collaboration (H. Aihara *et al.*), Phys. Rev. Lett. **57**, 404 (1986).
- [30] CELLO Collaboration (H.J. Behrend *et al.*), Z. Phys. C **56**, 381 (1992).
- [31] VENUS Collaboration (Fumiaki Yabuki *et al.*), J. Phys. Soc. Jap. **64**, 435 (1995).
- [32] ALEPH Collaboration (A. Heister *et al.*), Phys. Lett. B **569**, 140 (2003).
- [33] Belle Collaboration (H. Makazawa *et al.*), Phys. Lett. B **615**, 39 (2005).
- [34] J. Gasser, M.A. Ivanov, and N.E. Sainio, Nucl. Phys. B **745**, 84 (2006); hep-ph/0602234.
- [35] J. Bijnens and J. Prades, Nucl. Phys. B **490**, 239 (1997).
- [36] U. Bürgi, Nucl. Phys. B **479**, 392 (1997).
- [37] Yu.M. Antipov *et al.*, Phys. Lett. **B121**, 445 (1983).